Aggregation of POSS Monomers in Liquid Hexane: A Molecular-Simulation Study

Alberto Striolo,*,†,‡ Clare McCabe,‡ Peter T. Cummings,‡,§ Elaine R. Chan,||,⊥ and Sharon C. Glotzer||,#

School of Chemical Biological and Materials Engineering, The University of Oklahoma, Norman, Oklahoma 73019, Department of Chemical Engineering, Vanderbilt University, Nashville, Tennessee 37235-1604, Nanomaterials Theory Institute, Center for Nanophase Materials Sciences, Oak Ridge National Laboratory, Oak Ridge, Tennessee 37831-6494, and Department of Chemical Engineering and Department of Materials Science and Engineering, University of Michigan, Ann Arbor, Michigan 48109-2136

Received: March 2, 2007; In Final Form: May 4, 2007

Polyhedral oligomeric silsesquioxanes (POSS) are multifunctional molecules that can be employed as building blocks to develop nanocomposite materials whose mechanical properties often improve upon those of traditional polymeric materials. We report here molecular simulation results for the effective potential of mean force between octamethyl POSS monomers and between POSS monomers in which one methyl group has been substituted by a linear alkane chain of nine carbon atoms in liquid normal hexane at 300 and 400 K. The results are discussed and compared to available data for the effective interactions between octamethyl POSS monomers in normal hexadecane. Our results show that the effective short-ranged POSS−POSS attraction is significantly weaker in hexane than it is in hexadecane, perhaps explaining why normal hexane is often the solvent of choice for the preparation of POSS-containing materials. Additionally, we provide results for the radial distribution functions between selected sites in the POSS monomers that can be used both to understand the association between POSS monomers in solution and to parametrize coarse-grained simulation models. Such models will be used to study the formation of POSS-containing supramolecular structures such as lamellae or micelles that are currently not accessible by atomistic simulation and can be compared to experimental observations.

Introduction

Polyhedral oligomeric silsesquioxanes (POSS)[1] constitute a class of multifunctional molecules that hold enormous promise as building blocks for nanotechnological applications. POSS monomers are cages or cubes of silicon and oxygen atoms having the formula $R_8Si_8O_{12}$, where R is an organic or inorganic group that in the simplest possible case is a hydrogen atom. Because POSS chemistry is extremely flexible, a wide variety of organic functionalities, including alcohols, epoxides, esters, isocyanates, acrylates, silanes, and so forth,[2] can be grafted for one or all of the hydrogen atoms on the POSS cage. Naturally, different functional groups alter the physical properties of the cage (e.g., solubility of the monomer in common solvents[3,4]), and so a wide range of potential applications for POSS-based nanocomposites can be envisioned. For example, POSS molecules can be employed as additives in polymeric materials and in resins where they increase the resistance to heat and radiations and thus appear to be promising candidates for preparing coatings for space vessels (see ref 5 and the references therein). Recent reviews provide a detailed description of the many possible applications for POSS-containing materials,[6] as well as of the synthetic procedures that are currently employed for their manufacture.[7,8]

Despite this wealth of technological applications, little is known regarding the molecular mechanisms responsible for the changes in properties reported when POSS monomers are incorporated into various polymeric materials. Molecular simulations are an ideal tool for investigating these mechanisms, although POSS-containing systems are often too large for all-atom molecular simulation studies to be tractable. Among the available theoretical studies, Capaldi et al. have investigated the aggregation of POSS monomers within polymeric systems[9] and the mechanical properties of crystalline POSS monomers,[10] while Bharadwaj et al. have studied the structure of POSS-containing composites.[11] Although in this latter study the system investigated was relatively small, the results show clear evidence for aggregation between the POSS monomers.

In previous work, we employed molecular dynamics simulations to determine the effective pair potentials between POSS monomers dissolved, at dilute concentrations, in short poly(dimethyl siloxane) chains[12] and in normal hexadecane.[13] Our ultimate goal is to develop coarse-grained models to study systems containing a large amount of POSS monomers. These systems are intractable from an all-atom perspective with current computing power because of the system sizes needed and the time scale on which the phase transitions occur. Our previous results indicate that POSS monomers attract each other and that the attraction is strong, especially at short separations.[12,13]

* Author to whom correspondence should be addressed. Phone: 405 325 5716. Fax: 405 325 5813. E-mail: astriolo@ou.edu.
† The University of Oklahoma.
‡ Vanderbilt University.
§ Oak Ridge National Laboratory.
|| Department of Chemical Engineering, University of Michigan.
⊥ Present address: Electronics and Electrical Engineering Laboratory, Semiconductor Electronics Division, National Institute of Standards and Technology, Gaithersburg, MD 20899-8120.
Department of Materials Science and Engineering, University of Michigan.

10.1021/jp071730x CCC: $37.00
Published on Web 10/05/2007

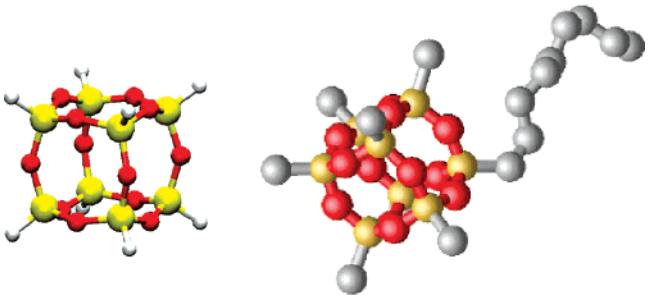

Figure 1. Schematic representation of the two POSS monomers considered in this work. On the left panel, we sketch the octa−methyl POSS; on the right one, we sketch the monotethered POSS monomer. In both panels, yellow spheres represent silicon atoms, red spheres are oxygen atoms, and white spheres are either methyl (CH_3) or methylene (CH_2) groups.

However, the effective pair potential can be manipulated by changing the temperature, the solvent, and especially the functionality of the R group tethered to the silicon atoms in the POSS cage. A recent molecular dynamics study by Pate et al.[14] indicates that by employing the latter strategy to control POSS monomer aggregation it is possible to manipulate the glass transition temperature of polymers. We also reported simulation results for telechelic POSS monomers dissolved in normal hexane,[15] which indicated that the backbone chain has a significant influence on both the equilibrium and the transport properties of the telechelic hybrid molecules. Normal hexane (nC$_6$) is often employed during the preparation of POSS-containing materials and is a low-molecular weight solvent that could be used in vapor pressure osmometry experiments to determine osmotic second virial coefficients between POSS monomers. Such experimental information, although not currently available, could be compared to the results presented here and used to validate our predictions.

In this manuscript, we report results obtained for the effective pair potential between POSS monomers dissolved in normal hexane (nC$_6$). The monomers of interest are the octamethyl POSS monomer used in our previous simulations, $(CH_3)_8Si_8O_{12}$, and the POSS monomer obtained from the octamethyl POSS when one CH_3 group is substituted with one linear alkane chain containing nine carbon atoms (referred hereafter as the monotethered POSS monomer). In Figure 1, we report a schematic representation of the two POSS monomers considered in this work.

Simulation Methods and Algorithms

Algorithms. The simulations were conducted in the NVT ensemble in which the number of molecules (N), the volume (V), and the system temperature (T) were maintained constant during each simulation run.[16] The simulation package DL-POLY[17] was employed to integrate the equations of motion. Rigid bonds are maintained using the SHAKE algorithm.[18] The simulation box is cubic and of size 6.0 nm. On the basis of our previous work in which we investigated system size effects, this box size is sufficiently large to eliminate system size effects on the results. We implemented periodic-boundary conditions in all three coordinate directions and maintained the temperature constant through the Nosé−Hoover thermostat using time constants of 0.5 or 1.0 ps.

Each system was prepared, as described elsewhere,[12,19] by first inserting the POSS monomers and then the solvent molecules in the simulation box. The number of nC$_6$ molecules (1100) dissolved in the 6.0 nm boxes is chosen to achieve a density similar to that of bulk liquid normal hexane at ambient conditions. The simulations were conducted at 300 and 400 K. Additional simulations were performed to assess the effect of pressure on the effective pair potentials between the POSS monomers, since, as the temperature increases in a constant volume ensemble, the pressure also increases. These simulations were conducted in the NPT ensemble in which the number of molecules (N), the pressure (P), and the temperature (T) are maintained constant. Because for a system with a fixed number of molecules at a given temperature the pressure increases as the volume decreases, to fix P, it is necessary to let V fluctuate. In our NPT simulations, the box size increased up to ∼6.5 nm (at 400 K) to reach ambient conditions P. The box volume then fluctuated above and below an approximately steady value.[16] At that point, NVT simulations were conducted to compute the radial distribution functions reported below with the volume fixed at the average value reached after the NPT simulations were concluded. To distinguish the latter simulations from those performed under NVT conditions, we will refer to them as the NPT simulations in the remainder of this work.

During the simulations, as described elsewhere,[12,13] we computed the radial distribution functions (RDFs) between the centers of mass of the POSS monomers. From these RDFs, it is possible to obtain a spherically symmetric quantity, $W(r)$, between the POSS monomers by applying the relation:[20]

$$\frac{W(r)}{kT} = -\ln[g(r)] \tag{1}$$

In eq 1, $g(r)$ is the RDF at a separation r between the centers of mass of two POSS monomers, k is the Boltzmann constant, and T is the absolute temperature. The quantity $W(r)$ is an effective pair potential of mean force (PMF).[20−22] From eq 1, we can see that a radial distribution function larger than unity determines an effective attraction between the monomers at a separation r between their centers of mass, while a radial distribution function less than unity determines an effective repulsion.

The results reported here are obtained as the average of 10 independent simulation runs. As in our previous studies, each production simulation run lasts 4.0 ns, and the system configurations are saved every 500 fs for statistical analysis.

Force Fields. Our previous ab initio studies show that it is possible to combine force fields originally developed to describe alkanes and silicon-based compounds to correctly predict the properties of hybrid organic/inorganic POSS monomers.[5,23] We demonstrated that by using such force fields it is possible to correctly predict, for example, the structure of POSS crystals.[24] On the basis of these findings, the POSS monomers are described here by implementing a force field originally developed to reproduce the radial distribution function of liquid poly(dimethyl siloxane).[25] The methyl groups are treated as united atoms.[26] Atoms in the same POSS monomer interact with each other via short-range potentials. Bond length fluctuations around the equilibrium separation r_0 are constrained by the bond stretching potential,

$$V_b(r) = k_b(r - r_0)^2 \tag{2}$$

Bond-angle oscillations about the equilibrium angle θ_0 are constrained by the bond bending potential,

$$V_a(\theta) = k_a(\theta - \theta_0)^2 \tag{3}$$

and torsional-angle fluctuations ϕ are constrained by a torsional potential given by,

$$V_t(\phi) = c_1[1 + \cos(\phi)] + c_2[1 - \cos(2\phi)] + c_3[1 + \cos(3\phi)] \quad (4)$$

In eqs 2, 3, and 4, V_b, V_a, and V_t are the bond length, angle, and torsional potentials respectively; k_b, k_a, c_1, c_2, and c_3 are proportionality constants; r, θ, and ϕ are the instantaneous bond length, bond angle, and torsional angle, respectively.

The alkane tether, composed of CH_2 and CH_3 united atom groups, is modeled according to the TraPPE united atom force field,[26] described later. To combine the force field used here to describe the POSS cages[25] with that used to describe the alkane backbone,[26] we require an appropriate algebraic description for the Si−CH_2 bond length, the O−Si−CH_2 and Si−CH_2−CH_2 bond angles, and the Si−O−Si−CH_2, O−Si−CH_2−CH_2, and Si−CH_2−CH_2−CH_2 torsional potentials. For consistency, we describe the Si−CH_2 bond length fluctuations with eq 2 employing the parameters used to describe the Si−CH_3 bond and describe the O−Si−CH_2 bond angle oscillations with eq 3. Following the COMPASS formalism,[27] we employ the following algebraic expression to describe the Si−CH_2−CH_2 bond angle fluctuations:

$$V_a(\theta) = k_a^I(\theta - \theta_0)^2 + k_a^{II}(\theta - \theta_0)^3 + k_a^{III}(\theta - \theta_0)^4 \quad (5)$$

The Si−O−Si−CH_2 potential was set equal to the Si−O−Si−CH_3 potential, and the Si−CH_2−CH_2−CH_2 torsion was set equal to that of CH_2−CH_2−CH_2−CH_2 in the TraPPE force field. To describe the O−Si−CH_2−CH_2 potential, we chose the CH_2−CH_2−CH_2−CH_2 potential from the TraPPE force field, with parameters set at half the original values, as described previously.[15]

In addition to intramolecular forces, Lennard−Jones 12-6 potentials describe the nonbonded CH_3−CH_3, CH_3−O, CH_2−Si, and CH_3−Si repulsive and dispersive interactions:

$$u(r_{ij}) = 4\epsilon_{ij}\left[\left(\frac{\sigma_{ij}}{r_{ij}}\right)^{12} - \left(\frac{\sigma_{ij}}{r_{ij}}\right)^{6}\right] \quad (6)$$

Lennard−Jones 9-6 potentials describe the nonbonded Si−O repulsive and dispersive interactions:

$$u(r_{ij}) = \epsilon_{ij}\left[2\left(\frac{\sigma_{ij}}{r_{ij}}\right)^{9} - 3\left(\frac{\sigma_{ij}}{r_{ij}}\right)^{6}\right] \quad (7)$$

In eqs 6 and 7, the parameters ϵ_{ij} and σ_{ij} have the usual meaning, and r_{ij} is the distance between atoms i and j. Nonbonded interactions between atoms in the same molecule are not accounted for unless the pairs of atoms are separated by more than three bonds, which is consistent with many formalisms, including the TraPPE force field.[26]

Normal hexane ($n$$C_6$) is described by the TraPPE united atom force field for alkanes,[26] in which the CH_3 and CH_2 groups are treated as single spherical interaction sites (i.e., the hydrogen atoms are not treated explicitly). The united atoms are linked through rigid bonds 0.154 nm in length. The fluctuations of bond angles and of dihedral angles are constrained through harmonic potentials of functional forms expressed by eqs 3 and 4, respectively. Nonbonded interactions between united atoms are treated within the Lennard−Jones 12-6 formalism, reported in eq 6. Interactions between dissimilar united atoms are determined from the Lorentz−Berthelot mixing rules. Nonbonded interactions between atoms in the same molecule are not accounted for unless the pairs of atoms are separated by more than three bonds. Nonbonded interactions between atoms belonging to POSS, the alkane tether, and the $n$$C_6$ solvent are treated according to the Lennard−Jones 12-6 formalism expressed in eq 6 with the appropriate choice of interaction parameters. In Table 1, we report the parameters required to implement the force fields used here.

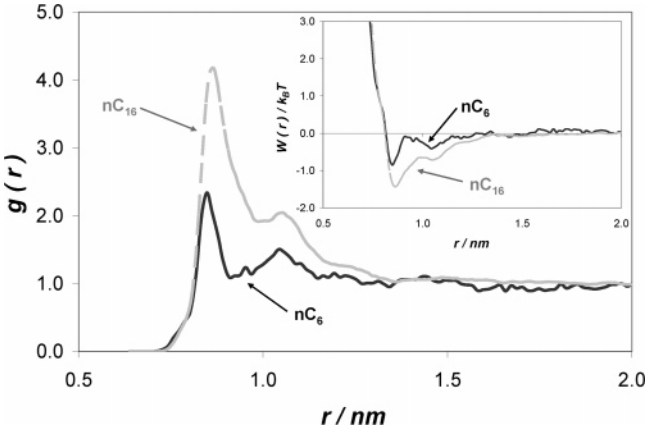

Figure 2. Radial distribution function and effective potential of mean force (inset) for $(CH_3)_8Si_8O_{12}$ POSS monomers dissolved in $n$$C_6$ (continuous black lines) and in $n$$C_{16}$ (broken gray lines) at 400 K. Results for POSS monomers in $n$$C_{16}$ are from ref 13.

Results

In Figure 2, we report molecular simulation results for the radial distribution function, RDF, and the effective potential of mean force, PMF (inset), between octamethyl POSS monomers in normal hexane ($n$$C_6$, black lines) at 300 K and compare the results to those obtained for the same POSS monomers dissolved in normal hexadecane ($n$$C_{16}$).[13] The definition of both RDF and PMF is provided in Simulation Methods and Algorithms. The RDF, and therefore also the effective PMF between the POSS monomers in $n$$C_6$, show a rather intense short-ranged attraction followed by a dip and a less intense attractive peak at intermediate separations. Our results do not provide evidence for intermediate repulsion, although the uncertainty connected with these calculations (see refs 12 and 13 for an estimation of such uncertainty) does not allow us to rule out this possibility. When we compare the effective pair potential to that obtained for octamethyl POSS monomers dissolved in normal hexadecane (gray lines), we note that the position of the peaks are the same in both solvents, although the peaks are significantly less pronounced in $n$$C_6$, and thus indicate a less intense effective attraction between POSS monomers in $n$$C_6$ than in $n$$C_{16}$. The effective attraction may be weaker in $n$$C_6$ because this solvent has a shorter chain than $n$$C_{16}$. Therefore, it is possible that hexadecane induces a depletion attraction between the POSS monomers.[19,28] Because the depletion attraction, a phenomenon of entropic origin, is expected to increase as the molecular weight of the alkane solvent molecules increases, it is more pronounced in $n$$C_{16}$ than in $n$$C_6$. The positions of the attractive peaks at short POSS−POSS separation in $n$$C_{16}$ were attributed in earlier work to the different relative orientations that the POSS monomers assume as they approach each other.[13] In particular, the peak at closest POSS−POSS separation was found to be due to a configuration in which two POSS monomers are in contact in a face-to-face configuration, while the peak at slightly larger separations is due to a configuration of the two approaching POSS monomers in which one corner of one monomer is near one corner of the second POSS monomer. The dip in

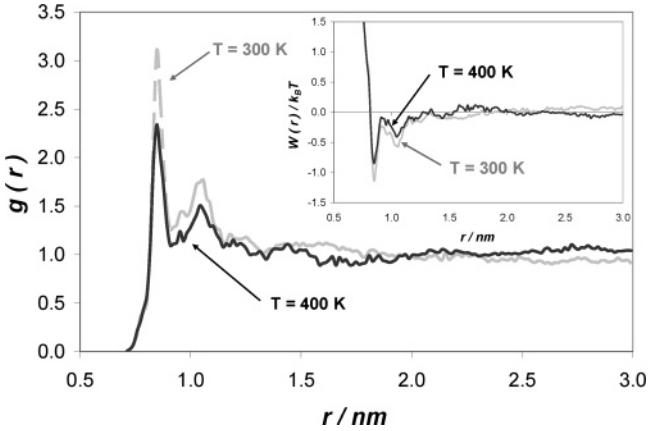

Figure 3. Radial distribution function and effective potential of mean force (inset) for $(CH_3)_8Si_8O_{12}$ POSS monomers dissolved in nC_6 at 300 K (broken gray lines) and at 400 K (continuous black lines). Both simulations are conducted in simulation boxes of the same volume (NVT ensemble).

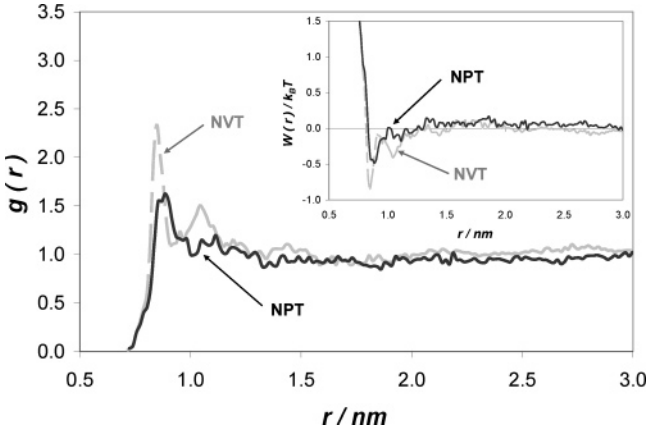

Figure 4. Radial distribution function and effective potential of mean force (inset) for $(CH_3)_8Si_8O_{12}$ POSS monomers dissolved in nC_6 at 400 K. Results are shown for NVT (broken gray lines) and NPT (continuous black lines) ensembles.

between the two attractive peaks was attributed to the penalty connected to the reorientation of the two approaching POSS monomers. Similar explanations hold for the effective interactions observed between octamethyl POSS monomers dissolved in nC_6 in this work.

In Figure 3, we report molecular simulation results for the RDF and the effective PMF (inset) between octamethyl POSS monomers in nC_6 at 300 K (broken gray lines) and 400 K (continuous black lines). The results do not show a significant temperature dependency, although the effective attraction between the two POSS monomers becomes weaker as the temperature increases, as would be expected because of the increased thermal motion at higher temperatures. The results reported in Figure 3 were obtained by conducting simulations in the NVT ensemble at both temperatures. When the volume is maintained constant but the temperature is increased, the system pressure necessarily increases. Consequently, the pressure for the system simulated at 400 K is larger than that for the system simulated at 300 K. To evaluate the effect of pressure on the effective pair potentials between the dissolved POSS monomers, we report in Figure 4 the RDF and the effective

TABLE 1: Potential Parameters for the Molecular Models Employed in This Work

bonds	r_0, Å	k_b, kcal/(mol Å^2)
Si−O	1.64	350.12
Si−CH_3	1.90	189.65
Si−CH_2	1.90	189.65

angles	θ_0, deg	k_θ, kcal/(mol rad^2)
Si−O−Si	146.46	14.14
O−Si−O	107.82	94.50
O−Si−CH_3	110.69	49.97
O−Si−CH_2	110.69	49.97
CH_3−CH_2−CH_2	114.00	62.09
CH_2−CH_2−CH_2	114.00	62.09

angles	θ_0, deg	k^{I}_θ, kcal/(mol rad^2)	k^{II}_θ, kcal/(mol rad^3)	k^{III}_θ, kcal/(mol rad^4)
Si−CH_2−CH_2	112.67	39.52	−7.44	0.00

dihedrals	c_1, kcal/mol	c_2, kcal/mol	c_3, kcal/mol
Si−O−Si−O	0.2250	0.0000	0.0000
Si−O−Si−CH_3	0.0000	0.0000	0.0100
Si−O−Si−CH_2	0.0000	0.0000	0.0100
O−Si−CH_2−CH_2	0.3527	−0.0677	0.7862
Si−CH_2−CH_2−CH_2	0.7054	−0.1355	1.5724
CH_3−CH_2−CH_2−CH_2	0.7054	−0.1355	1.5724
CH_2−CH_2−CH_2−CH_2	0.7054	−0.1355	1.5724

nonbonded interactions	σ_{ij}, Å	ϵ_{ij}, kcal/mol
Si−Si	4.29	0.1310
O−O	3.30	0.0800
Si−O	3.94	0.0772
CH_3−CH_3	3.75	0.1947
CH_2−CH_2	3.95	0.0974
CH_3−CH_2	3.85	0.1377
Si−CH_3	3.83	0.1596
Si−CH_2	3.93	0.1093
O−CH_3	3.38	0.1247
O−CH_2	3.48	0.0854

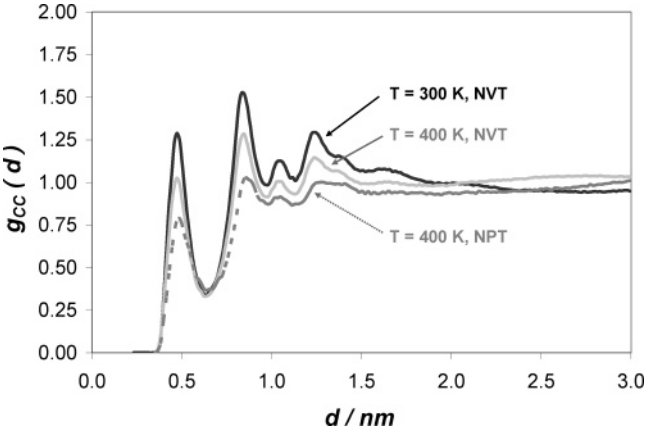

Figure 5. Corner−corner radial distribution function, $g_{CC}(d)$, computed between the corners of the $(CH_3)_8Si_8O_{12}$ POSS monomers dissolved in nC_6. Results are shown at 300 K (continuous black line), at 400 K in the NVT ensemble (continuous gray line), and at 400 K in the NPT ensemble (dotted gray line).

PMF (inset) between octamethyl POSS monomers in nC_6 at 400 K. The results were obtained in the NVT (broken gray lines) and NPT ensemble (continuous black lines). We find that, given the statistical uncertainty of our calculations, the results are not very different. However, we note that both of the attractive short-ranged peaks in the RDF observed in the NVT ensemble become somewhat less pronounced when the simulations are conducted within the NPT ensemble. This result may be due to solvent-related excluded-volume effects which become more pronounced as the pressure increases. However, because of the symmetry of the POSS monomers employed in these simulations, these effects are almost negligible given the precision of our calculations. We expect these effects to become more noticeable as the symmetry of the POSS monomers is lost, as, for example, when monotethered POSS monomers are considered.

To better appreciate the structure of the POSS aggregates in the system, we computed the radial distribution function between the corners of the octamethyl POSS monomers dissolved in nC_6. The corner sites are located in the middle of the bond that connects each silicon atom in the POSS cage to the nearest methyl group (as reported within). The corner−corner radial distribution function was computed between sites that do not belong to the same POSS monomer. In Figure 5, we report the corner−corner RDF at 300 K (continuous black line) and 400 K in the NVT ensemble (continuous light gray line) and at 400 K in the NPT ensemble (lower pressure, dotted dark gray line). In all cases, our results show many peaks which are due to the rigid nature of the POSS cube. The effect of increasing temperature is reflected in a decrease of each of the peaks and is enhanced when we compare results at 300 and 400 K at the same pressure (continuous black and dotted dark gray lines, respectively). Only in this latter case do peaks that are larger than unity at 300 K become lower than unity at 400 K. Generally, RDFs larger than unity indicate effective attractions, and RDFs lower than unity indicate effective repulsions; thus, this information should be considered when coarse-grained models are derived for POSS monomers dissolved in organic solvents. It is instructive to note that the position of the peaks does not change as either temperature or pressure are manipulated. This result is probably due to the rigid structure of the POSS monomers considered in this study[23,24] and provides support for previous coarse-grained simulations in which POSS monomers are represented as rigid cubes[29−30,31] and single interaction sites.[32]

Thus far, we have investigated the behavior of symmetric POSS monomers dissolved in common organic solvents. In symmetric POSS monomers, each functional group R is characterized by the same chemical composition (in our case, each R was a methyl group). In many cases of practical interest, one R group can be different from the other seven. The particular R group can, for example, be used to attach the POSS monomer to a polymer or provide a specific functional moiety (e.g., water-soluble tether) while the other seven groups confer solubility to the compound in a given solvent. To understand the effect of introducing asymmetry into the POSS monomers on the effective pair potentials, we compare in Figure 6 the RDF and the effective PMF (insets) between POSS monomers in nC_6 at 300 (top) and 400 K (bottom). The results are for octamethyl POSS monomers (gray lines) and for monotethered POSS monomers (black lines). All results are obtained in the NVT ensemble.

At 300 K, the results for both RDF and PMF shown in Figure 6 indicate that, qualitatively, the presence of the tether does not significantly affect the simulated pair interactions. When one methyl group is substituted with a short alkane chain, the first attractive peak observed in the RDF, and hence in the related effective PMF, becomes less intense and wider, and the attractive shoulder becomes more intense. We also observe that the RDF calculated between monotethered POSS monomers is nonzero at $r \sim 0.7$ nm, at which center of mass separation the RDF between the octamethyl POSS monomers is zero. This result is due to the presence of the tether which effectively moves the center of mass from the center of the rigid POSS cage (where it is located in the case of octamethyl POSS) to its periphery. Because the center of mass does not reside at the center of the POSS cage, it is possible that the centers of mass of two approaching monotethered POSS monomers can be found at shorter separations compared with those for octamethyl POSS monomers. The presence of the alkane tether is also responsible for introducing a long-ranged weak attraction between the monotethered POSS monomers. This result was unexpected and is probably due to solvent-related excluded-volume effects.

More interesting is the comparison of the results obtained at 400 K (Figure 6, bottom). While our simulations predict an effective short-ranged attraction between the octamethyl POSS monomers, the effective pair potential between the monotethered POSS monomers indicates a short-ranged repulsion followed by a weak mid-ranged attraction. The intensity of the mid-ranged attraction is comparable to the accuracy of our calculations and so may not be present in practice. The short-ranged repulsion becomes more pronounced as the distance between the centers of mass of two approaching monotethered POSS monomers decreases. This type of short-ranged repulsion is often observed for colloidal brushes in solution and is due to entropic effects.[33−35]

The results shown in Figure 6 indicate that at 400 K the entropic effects prevail over other types of interactions (e.g., specific interactions between the POSS monomers or solvent-related excluded-volume effects) that appear responsible for the attraction observed between the monotethered POSS monomers in nC_6 at 300 K. Because we expected the entropic repulsion to arise even at 300 K, we conducted additional simulations for the monotethered POSS monomers dissolved in nC_6 in the NPT ensemble (lower pressure) at both 300 and 400 K.

We report in Figure 7 the results for the RDF and the effective PMF (inset) between the monotethered POSS monomers at 300 K (top) and at 400 K (bottom). If we compare the results obtained in the NVT ensemble (pressure above room conditions,

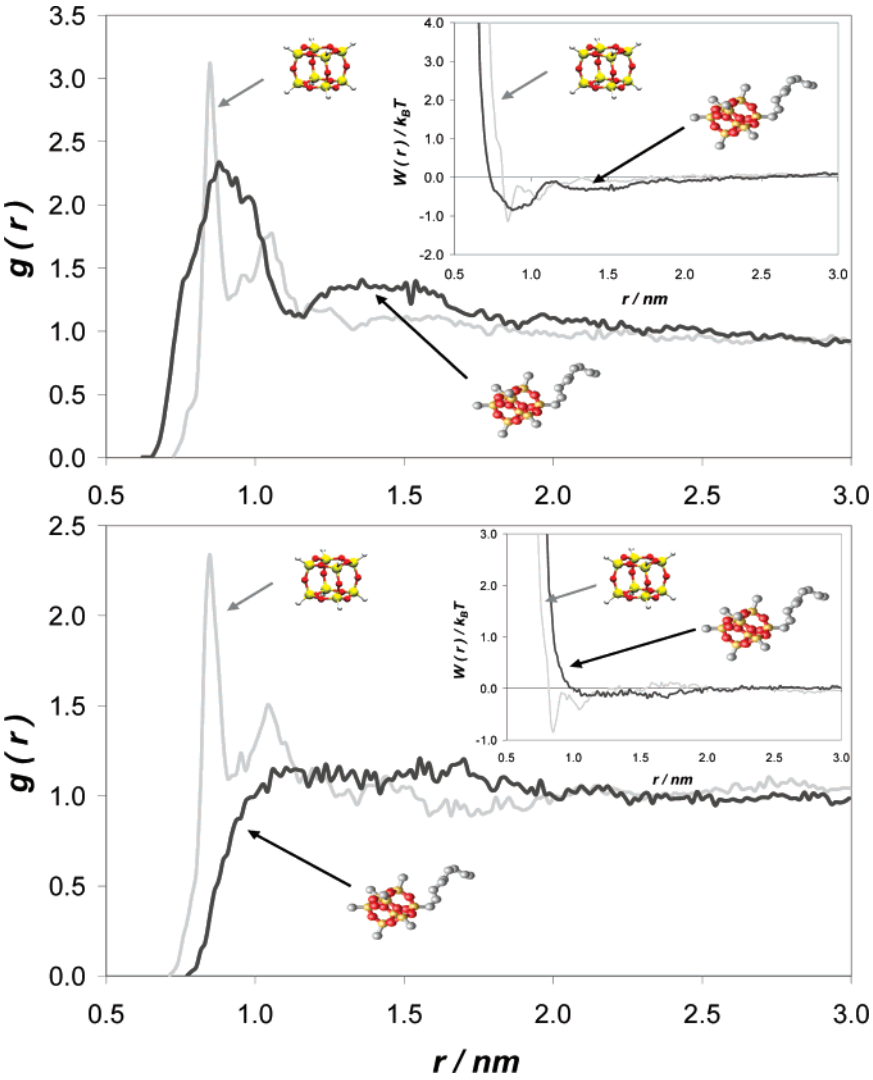

Figure 6. Radial distribution function and effective potential of mean force (inset) for POSS monomers dissolved in nC_6. Results are for $(CH_3)_8$-Si_8O_{12} (continuous gray lines) and for monotethered POSS monomers (continuous black lines). Simulations were conducted at 300 K (top panel) and at 400 K (bottom panel). Results at 400 K are those obtained in the NVT ensemble.

gray lines) to those obtained in the NPT ensemble (room condition pressure, black lines), we observe that at 400 K the effect of pressure is negligible; the only difference between the RDFs at 400 K is that the weak mid-ranged attraction observed in the NVT ensemble became shorter-ranged in the NPT one. However, at 300 K, we notice that the intense short-ranged attraction between the monotethered POSS monomers observed in the NVT ensemble (large pressure) completely disappears in the results obtained in the NPT one (ambient conditions). This latter result reveals that the entropic effects discussed above are significant even at 300 K but that these effects can be reduced by increasing the pressure of the system. Increasing the pressure probably induces solvent-related excluded-volume effects that effectively force the POSS monomers to aggregate. Such effects should be considered if the results discussed here were to be used in developing coarse-grained models. Namely, coarse-grained models obtained at ambient pressures may not be reliable to conduct simulations at larger pressures. To develop such models, one could employ radial distribution functions between selected sites in the molecular dynamics simulations discussed here to develop ad hoc site−site effective potentials.[36−39]

To permit the derivation of these site−site effective potentials,[22] we calculated radial distribution functions between selected sites in the monotethered POSS monomers dissolved in nC_6. In Figure 8, we report a schematic description of three sites defined by the coordinates of one monotethered POSS monomer: corner, tether, and end. The corner site is defined as the midpoint between each silicon atom in the POSS cage and its nearest CH_3 or CH_2 group. The tether site is defined as the midpoint between two consecutive CH_2 groups in the tether attached to the POSS cage. The end site is defined as the midpoint between the last CH_2 group in the tether and the final CH_3 group. Each monotethered POSS monomer is determined by eight corner sites, three tether sites, and one end site. The tether sites are located between the second and third, fourth and fifth, and sixth and seventh carbon atoms in the tether, where the first carbon atom is the one chemically bound to the silicon atom of the POSS cage.

We calculated corner−corner (continuous black lines), tether−tether (continuous light gray lines), and end−end (dotted dark gray lines) RDFs by only considering sites belonging to different POSS monomers. In Figure 9, we report the results obtained at 300 K, and in Figure 10, we report those obtained at 400 K. In both figures, the top panel is for results obtained in the NVT ensemble and the bottom panel for those obtained in the NPT ensemble. In all cases considered, the corner−corner RDFs (continuous black lines) show many peaks. As discussed above for octamethyl POSS monomers dissolved in nC_6 (see Figure

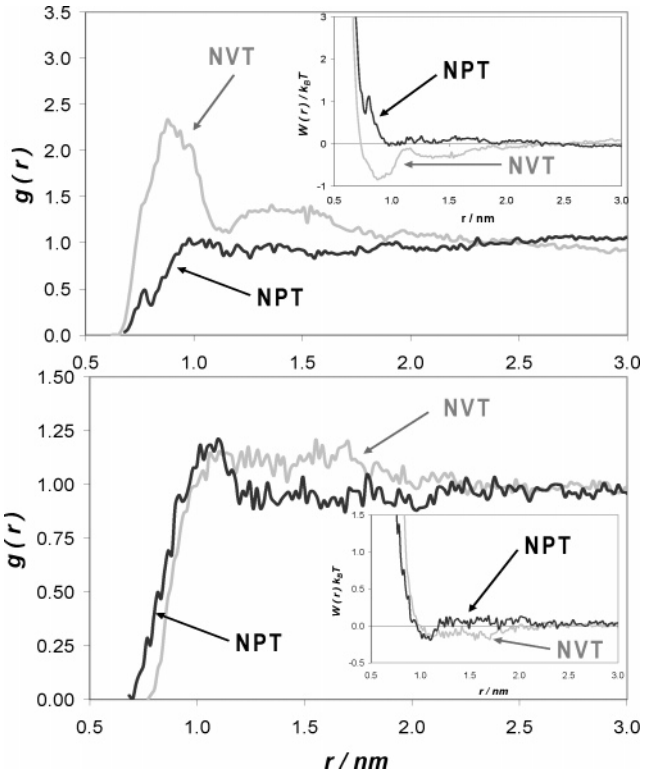

Figure 7. Radial distribution function and effective potential of mean force (inset) for monotethered POSS monomers dissolved in nC$_6$ at 300 K (top panel) and at 400 K (bottom panel). Results are obtained in the NVT (continuous gray lines) or in the NPT ensemble (continuous black lines).

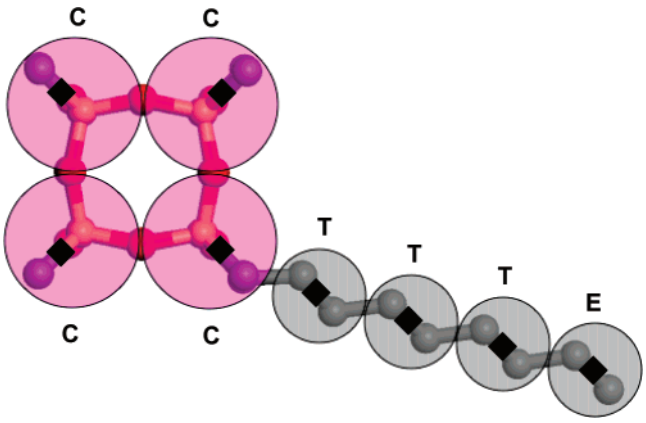

Figure 8. Schematic representation of the sites considered in computing corner−corner, tether−tether, and end−end radial distribution functions. The black diamonds highlight the positions of the sites. C is for corner site, T for tether site, and E for end site.

5), these peaks are due to the rigid cubic structure of the POSS cage. As described elsewhere,[23] the presence of the alkane tether does not deform the cubic rigid structure of the POSS cage. It is interesting to note that the peaks are larger than unity only for the case of monotethered POSS monomers dissolved in nC$_6$ at 300 K in the NVT ensemble (Figure 9, top panel). This observation is due to the effective attraction between the POSS monomers in this case (see Figure 7, top panel). In all other cases, an effective repulsion is observed between the monotethered POSS monomers, and this repulsion is manifested in the corner−corner RDFs by peaks at close separations that are lower than unity. The tether−tether RDFs (continuous light gray lines) in general do not show narrow peaks. In all cases, except at 300 K in the NVT ensemble (Figure 9, top panel), these RDFs

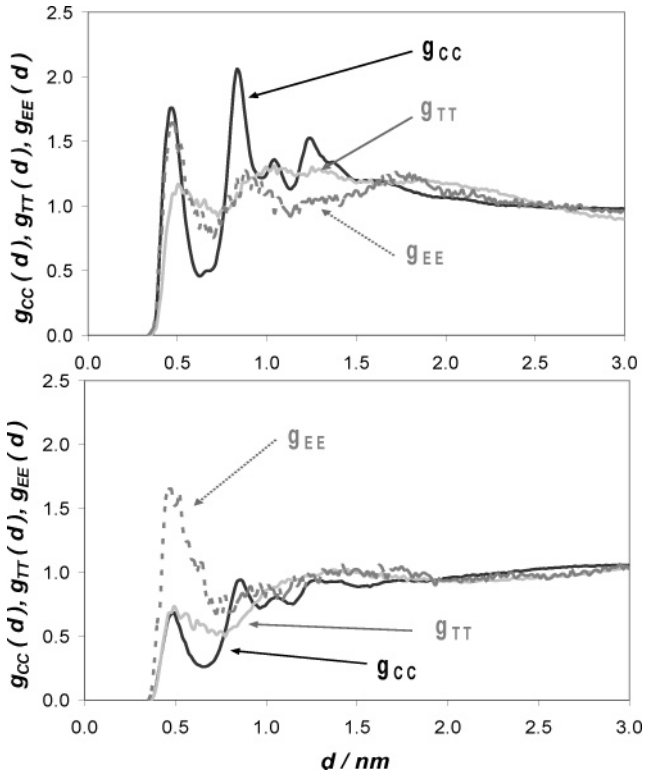

Figure 9. Corner−corner (g_{CC}, continuous black lines), tether−tether (g_{TT}, continuous gray lines), and end−end (g_{EE}, dotted gray lines) radial distribution functions computed for monotethered POSS monomers dissolved in nC$_6$ at 300 K. The top panel is for data collected in the NVT ensemble; the bottom is for those obtained in the NPT ensemble.

are lower than unity at close separations, suggesting an effective repulsion between the tethers that is probably due to entropic reasons. At 300 K in the NVT ensemble (Figure 9, top panel), the tether−tether RDF is larger than unity at intermediate separations. This feature is probably related to the effective mid-ranged attraction observed between monotethered POSS monomers in nC$_6$ at 300 K in the NVT ensemble (see Figure 7, top panel). This suggests that tether−tether association may be responsible for that effective attraction. The tether−tether association is probably due to solvent-related excluded-volume effects. The end−end RDFs (dotted dark gray lines) are more complex. Both at 300 and at 400 K in the NVT ensemble (top panels of Figures 9 and 10, respectively), these RDFs show two peaks larger than unity at small separations, followed by oscillations near unity at larger separations. The separation between the two peaks is ∼0.4−0.5 nm larger at higher temperatures but similar to the diameter of one CH_2 or CH_3 group. These observations suggest that the end of the tethers can in some cases approach each other, although tether segments in general cannot (see continuous light gray lines), and that perhaps one solvent segment sometimes separates two approaching end segments. This is not too surprising given that the chemistry of the nC$_6$ solvent is the same as that of the tether in the monotethered POSS monomer. In the NPT ensemble (room condition pressure) both at 300 and at 400 K (bottom panels in Figures 9 and 10, respectively), the second peak larger than unity in the end−end RDFs practically disappears, as expected because the simulated system is less crowded at lower pressures than at higher pressures.

Although the site−site RDFs just discussed cannot be directly employed to extract site−site effective potentials for coarse-grained simulations in which the solvent is treated implicitly, they can be used in iterative schemes to obtain effective

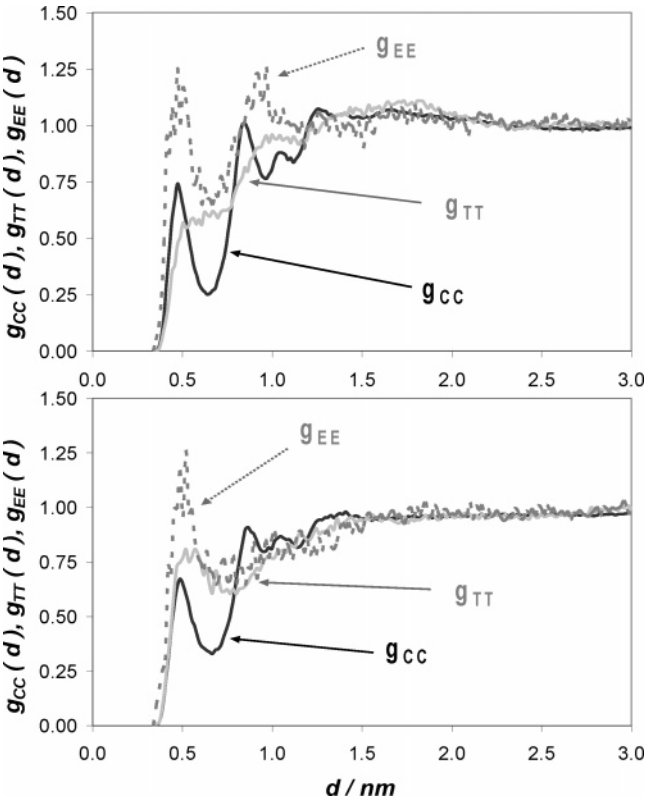

Figure 10. Corner−corner (g_{CC}, continuous black lines), tether−tether (g_{TT}, continuous gray lines), and end−end (g_{EE}, dotted gray lines) radial distribution functions computed for monotethered POSS monomers dissolved in nC$_6$ at 400 K. The top panel is for data collected in the NVT ensemble; the bottom is for those obtained in the NPT ensemble.

potentials.[22] Further, the site−site RDFs are useful for understanding the molecular mechanisms responsible for the association between POSS monomers in various solvents.

Conclusions

We have reported equilibrium molecular dynamics simulation results for polyhedral oligomeric silsesquioxane monomers dissolved in liquid normal hexane at 300 K and at 400 K. We considered one symmetric POSS monomer (octamethyl POSS) and one monotethered POSS monomer in which one of the methyl groups was substituted by one linear hydrocarbon chain of nine carbon atoms. We have obtained effective pair potentials of mean force between the POSS monomers at dilute concentration and compared our results to those previously obtained for octamethyl POSS monomers in normal hexadecane. Although we observe an effective attraction between the octamethyl POSS monomers at short separation between their centers of mass, this attraction is significantly weaker compared with that reported between similar POSS monomers in normal hexadecane. This result may explain why normal hexane is often the solvent of choice in the experimental preparation of POSS-containing materials.

The introduction of the tether in the POSS monomer significantly alters the features of the effective pair potentials. In particular, we observe the appearance of a short-ranged effective repulsion which is probably due to entropic effects.

We also reported results for site−site radial distribution functions that could be useful in the implementation of coarse-grained models for the simulation of POSS monomer aggregation to study supramolecular structures such as lamellae or micelles. We point out that molecular simulation results strongly depend on the accuracy of the force fields employed to describe both inter- and intramolecular interactions. Care was taken, in our previous work, to validate the force fields used here by comparison both to the experimental structure of the perfect POSS crystals[24] and to the ab initio data obtained for single POSS monomers.[23] Although no experimental data is currently available to directly validate the simulation results presented here, we expect that a qualitative corroboration could be obtained once coarse-grained models are developed.[22]

Acknowledgment. The authors acknowledge financial support from the U.S. National Science Foundation through a Nanotechnology Interdisciplinary Research Team (NIRT) award, DMR-0103399. A.S. gratefully acknowledges financial support from the Vice President for Research at the University of Oklahoma through a Junior Faculty Research Program award. Calculations were performed on the VAMPIRE cluster at Vanderbilt University.

References and Notes

(1) POSS is a trademark of Hybrid Plastics, www.hybridplastics.com.
(2) Shockey, E. G.; Bolf, A. G.; Jones, P. F.; Schwab, J. J.; Chaffee, K. P.; Haddad, T. S.; Lichtenhan, J. D. *Appl. Organomet. Chem*. **1999**, *13*, 311.
(3) Lichtenhan, J. D. *Commun. Inorg. Chem*. **1995**, *17*, 115.
(4) Schockey, E. G.; Bolf, A. G.; Jones, P. F.; Schwab, J. J.; Chaffee, K. P.; Haddad, T. S.; Lichtenhan, J. D. *Appl. Organomet. Chem.* **1999**, *13*, 311.
(5) McCabe, C.; Glotzer, S. C.; Kieffer, J.; Neurock, M.; Cummings, P. T. *J. Theor. Comput. Chem.* **2004**, *1*, 265.
(6) Phillips, S. H.; Haddad, T. S.; Tomczak, S. J. *Curr. Opin. Solid State Mater. Sci.* **2004**, *8*, 21.
(7) Kopesky, E. T.; Haddad, T. S.; Cohen, R. E.; Mckinley, G. H. *Macromolecules* **2004**, *37*, 8992.
(8) Pyun, J.; Matyjaszewski, K.; Wu, J.; Kim, G.-M.; Chun, S. B.; Mather, P. T. *Polymer* **2003**, *44*, 2739.
(9) Capaldi, F. M.; Rutledge, G. C.; Boyce, M. C. *Macromolecules* **2005**, *38*, 6700.
(10) Capaldi, F. M.; Boyce, M. C.; Rutledge, G. C. *J. Chem. Phys*. **2006**, *124*, 214709.
(11) Bharadwaj, R. K.; Berry, R. J.; Farmer, B. L. *Polymer* **2000**, *41*, 7209.
(12) Striolo, A.; McCabe, C.; Cummings, P. T. *J. Phys. Chem. B* **2005**, *109*, 14300.
(13) Striolo, A.; McCabe, C.; Cummings, P. T. *Macromolecules* **2005**, *38*, 8950.
(14) Patel, R. R.; Mohauraj, R.; Pittman, C. U., Jr. *J. Polym. Sci., Part B: Polym. Phys.* **2006**, *44*, 234.
(15) Striolo, A.; McCabe, C.; Cummings, P. T. *J. Chem. Phys*. **2006**, *125*, 104904.
(16) Allen M. P.; Tildesley, D. J. *Computer Simulation of Liquids;* Oxford University Press: New York, 1987.
(17) Smith W.; Forester, T. *J. Mol. Graphics* **1996**, *14*, 136.
(18) Darden, T.; York, D.; Pedersen, L. *J. Chem. Phys.* **1993**, *98*, 10089.
(19) Striolo, A.; Colina, C. M.; Elvassore, N.; Gubbins, K. E.; Lue, L. *Mol. Simul*. **2004**, *30*, 437.
(20) Chandler, D. *Introduction to Modern Statistical Mechanics;* Oxford University Press: New York, 1987.
(21) Tavares, F. W.; Bratko, D.; Striolo, A.; Blanch, H. W.; Prausnitz, J. M. *J. Chem. Phys*. **2004**, *120*, 9859.
(22) Chan, E. R.; Striolo, A.; McCabe, C.; Glotzer, S. C.; Cummings, P. T., submitted.
(23) Li, H.-C.; Lee, C. Y.; McCabe, C.; Striolo, A.; Neurock, M. *J. Phys. Chem. A* **2007**, *111*, 3577.
(24) Ionescu, T. C.; Qi, F.; McCabe, C.; Striolo, A.; Kieffer, J.; Cummings, P. T. *J. Phys. Chem. B* **2006**, *110*, 2502.
(25) Frischknecht, A. L.; Curro, J. G. *Macromolecules* **2003**, *36*, 2122.
(26) Martin, M. G.; Siepmann, J. I. *J. Phys. Chem. B* **1998**, *102*, 2569.
(27) Sun, H. *Macromolecules* **1995**, *28*, 701.
(28) Asakura, S.; Oosawa, F. *J. Chem. Phys.* **1954**, *22*, 1255.
(29) Chan, E. R.; Zhang, X.; Lee, C.-Y.; Neurock, M.; Glotzer, S. C. *Macromolecules* **2005**, *38*, 6168.
(30) Zhang, X.; Chan, E. R.; Glotzer, S. C. *J. Chem. Phys*. **2005**, *123*, 184718.
(31) Chan, E. R.; Ho, L.; Glotzer, S. C. *J. Chem. Phys*. **2006**, *125*, 064905.
(32) Peng, Y.; McCabe, C. *Mol. Phys.* **2007**, *105*, 261.

(33) Matsen, M. W. *Macromolecules* **2005**, *38*, 4525.
(34) Matsen, M. W. *Phys. Rev. Lett.* **2005**, *95*, 069801.
(35) Striolo, A. *Phys. Rev. E: Stat. Phys., Plasmas, Fluids, Relat. Interdiscip. Top.* **2006**, *74*, 041401.
(36) Lyubartsev, A. P.; Laaksonen, A. *Phys. Rev. E: Stat. Phys., Plasmas, Fluids, Relat. Interdiscip. Top.* **1995**, *52*, 3730.
(37) Soper, A. K. *Chem. Phys*. **1996**, *202*, 295.
(38) Tschop, W.; Kremer, K.; Batoulis, J.; Burger, T.; Hahn, O. *Acta Polym.* **1998**, *49*, 61.
(39) Reith, D.; Putz, M.; Muller-Plathe, F. *J. Comput. Chem*. **2003**, *24*, 1624.